Spontaneous Iodide Activation at the Air-Water Interface of Aqueous Droplets

Yunlong Guo, Kangwei Li, Sébastien Perrier, Taicheng An, D. Donaldson, C. George

Spontaneous iodide activation at the air-water interface of aqueous droplets

Yunlong Guo[1,2#], Kangwei Li[2,3#,*], Sebastien Perrier[2], Taicheng An[1,*], D. James Donaldson[4,*], Christian George[2,*]

[1] Guangdong Key Laboratory of Environmental Catalysis and Health Risk Control, Guangdong-Hong Kong-Macao Joint Laboratory for Contaminants Exposure and Health, School of Environmental Science and Engineering, Institute of Environmental Health and Pollution Control, Guangdong University of Technology, Guangzhou 510006, China

[2] Univ Lyon, Université Claude Bernard Lyon 1, CNRS, IRCELYON, F-69626, Villeurbanne, France

[3] Department of Environmental Sciences, University of Basel, 4056, Basel, Switzerland

[4] Department of Chemistry, University of Toronto, 80 St. George Street, Toronto, Ontario M5S 3H6, Canada

*** Correspondence to:**
Kangwei Li (kangwei.li@unibas.ch)
Taicheng An (antc99@gdut.edu.cn)
D. James Donaldson (james.donaldson@utoronto.ca)
Christian George (christian.george@ircelyon.univ-lyon1.fr)

# These authors contributed equally to this work

Abstract

We present experimental evidence that atomic and molecular iodine, I and I_2, are produced spontaneously in the dark at the air-water interface of iodide-containing droplets without any added catalysts, oxidants or irradiation. Specifically, we observe I_3^- formation within droplets, and I_2 emission into the gas phase from NaI-containing droplets over a range of droplet sizes in this laboratory study. The formation of both products is enhanced in the presence of electron scavengers, either in the gas phase or in solution, and clearly follows a Langmuir−Hinshelwood mechanism, suggesting an interfacial process. These observations are consistent with iodide oxidation at the interface, possibly initiated by the strong intrinsic electric field present there, followed by well-known solution-phase reactions of the iodine atom. This interfacial chemistry could be important in many contexts, including atmospheric aerosols.

Keywords: spontaneous iodide activation, air−water interface, iodine, aqueous droplets, atmospheric chemistry

Synopsis: Spontaneous interfacial production of I and I_2 is observed in iodide-containing aerosol droplets. This suggests a previously unknown source of reactive iodine species and could be important in atmospheric marine environment.

Table of Contents (TOC)/Abstract Graphic

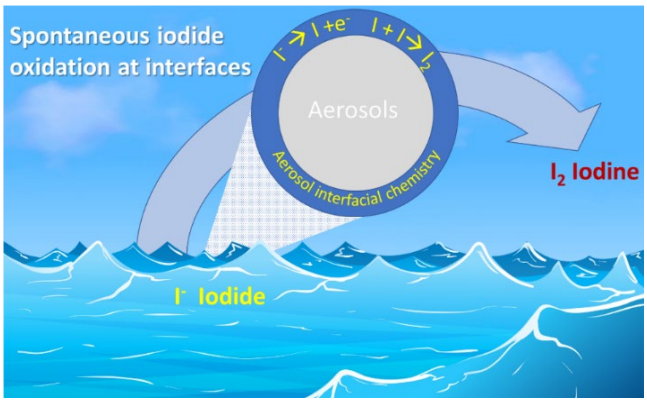

Introduction

Aerosols and cloud droplets are key and ubiquitous components in the atmospheric system, presenting a large air-water interface in the atmosphere.[1,2] Many species display a minimum free-energy at the air-water interface of such droplets, thus creating a favored and unique environment for chemical reactions.[3,4] Very recently, it has been found that spontaneous H_2O_2 and OH radical generation and reduction of organic compounds take place at the air-water interface of microdroplets,[5–9] while those reactions do not occur spontaneously in bulk solution. These intriguing phenomena observed from microdroplets do not rely on additional catalysts, external voltages, reducing agent, oxidants or irradiation, which have received great attention in recent years and were intensively debated.[10–12] In a recent study by Li et al.,[9] an attempt was made to finally recombine all previous observations by underlying the fact that the appearance of such oxidants is not resulting from an oxidation process, but rather a charge separation process involving the ion-neutral pair of OH^-. As initially suggested by Kloss,[13] such interfacial reactivity may be driven by the intrinsic electric field (strength reported at the order of $\sim 10^9$ V m^{-1}) existing at the air-water interface of microdroplets, which is suspected to be strong enough to induce charge separation in ion-pairs or facilitate certain reactions by reducing the activation energy.[14–16]

Molecular iodine (I_2) plays a key role in various important atmospheric cycles,[17,18] especially in marine environments. Iodine photochemistry has been shown to drive new particle formation in the marine boundary layer,[19,20] and to reduce global ozone levels by ca. 15%.[21] Recently, it has been shown that I_2 injections into the stratosphere may even represent a small but non-negligible process inducing O_3 depletion.[22] Gas phase I_2 in the marine environment originates from various sources such as photodissociation of organo-iodine in tidal and open ocean areas, as well as the direct I_2 release from biota near the coastal areas.[23–25] Currently, the reaction between ozone and iodide anions is believed to dominate abiotic atmospheric iodine production.[18,26,27]

Here we report a novel mechanism for I_2 production at the air-water interface of submicron and micron-sized NaI-containing droplets. Both gas phase I_2 and solution phase I_3^- are experimentally observed in the dark, in the absence of ozone. A very recent publication has also reported on solution-phase I_3^- production (though not gas phase products) within droplets;[28] the present work provides strong evidence that both $I_{3(aq)}^-$ and $I_{2(g)}$ are products of the same water surface-mediated dark oxidation of iodide ions. The spontaneous formation of gas phase I_2, although perhaps not environmentally significant on Earth due to the low iodide amounts in actual seawater (I^- concentration of 10−200 nM),[24,29] nevertheless represents another example of redox chemistry that is mediated by the high potentials present at the air-water interface of aqueous droplets.

Materials and Methods

Quantification of I_3^-

UV-Vis absorption spectra of I^-, $I_{2(aq)}$ and I_3^- standard solutions were measured over a relevant range of concentrations. The I_3^- standard solution was prepared by adding large excess of NaI to a solution with known amount of $I_{2(aq)}$; due to the large equilibrium constant for I_3^- formation, the initial $I_{2(aq)}$ was assumed to fully convert to I_3^- (see Text S1−S2). As shown in Figure 1A, the absorption peaks for these three species can be identified and clearly distinguished; the I_3^- showed clear absorption peaks at ~288 and ~352 nm respectively, consistent with previous literature.[30,31] Using the absorption intensity at 352 nm with a molar absorptivity of $2.38 \pm 0.056 \times 10^4$ L cm^{-1} mol^{-1} (Figure S1 and Text S2), the I_3^- concentration could be quantified, with the quantification limit at ~0.20 μM.

Mist chamber and atomizer experiments

The home-made mist chamber has been reported in our recent study[9] and is shown in Figure S2A. It has a volume of ~110 mL. When the gas flow goes through the mist chamber, the reservoir solution at the bottom will be lifted up due to pressure difference and therefore microdroplets are continuously sprayed out. Such microdroplets impacted a hydrophobic PTFE membrane filter (0.2 μm pore size, Ref: FGLP04700, Merck Millipore Ltd) mounted at the top of the mist chamber, and then dropped back into the bulk solution for respraying. As shown in Figure S2C, we measured the microdroplet number size distribution (APS, TSI 3321) at the outlet of mist chamber during the spraying process, and no particles were observed when a membrane filter was added. For a typical mist chamber experiment, 20 mL bulk NaI solution was added and the total gas flow was adjusted by mass flow controllers at 2.5 L min^{-1}. $C_2H_4ClOH_{(g)}$, as an electron scavenger with a pKa value of 14.31,[32] was generated by a gentle N_2 flow passing through the headspace of a 120 mL bottle filled with 30 mL pure C_2H_4ClOH solution, and the $C_2H_4ClOH_{(g)}$ concentration was calculated based on its vapor pressure. It is expected that the solution in the mist chamber evaporated continuously during the spraying process, and the remaining volume of solution decreased gradually overtime. We calculated the liquid loss rate for each individual experiment, with the range of 1.7−2.6 mL h^{-1} (Tables S1−S2). For these electron-scavenging experiments using C_2H_4ClOH, the solution pH decreased to 1−2 due HCl formation through hydrolysis of the dissolved $C_2H_4ClOH_{(g)}$. Previous studies have shown important role of solution acidity for I_2 production, and iodide activation is favored at lower solution pH.[33,34] Additionally, we performed macroscopic

aqueous interfacial experiments as shown in Figure S6, and see whether spontaneous iodide activation can occur on flat macroscopic surfaces in the dark.

We also produced iodide-containing droplets by atomizing bulk NaI solution using a commercial constant output atomizer (TSI 3076) (Figure S2B), which is a different spraying procedure compared with the mist chamber. Since both spraying procedures used the same bulk NaI solution, we assumed that the composition of the droplets generated from atomizer are the same with microdroplets generated from mist chamber. The droplets produced in the atomizer passed through two tandem 5 L glass bottles, where some large droplets were condensed and collected for UV-Vis measurement. Note that we continuously atomized the bulk solution for about 20 h, until enough solution (i.e., 2−3 mL) accumulated in these bottles to be transferred into a quartz cuvette for UV-Vis analysis. Although such atomizers are mostly used for generating small droplets in the submicron range (Figure S2E), micron-sized droplets are still produced, but with much lower number concentrations. As shown in Figure S2D, we measured the size distributions of microdroplets produced by such an atomizer, which typically peaked at ~2 μm diameter with a broad size range.

Gas-phase $I_{2(g)}$ measurement with CI-Orbitrap

Bromide chemical ionization mass spectrometry (Br-CIMS) has been frequently deployed to directly measure gas-phase iodine species, where dibromomethane (CH_2Br_2) is used to produce bromide as reagent ions due to its good affinity to various iodine species.[25,35] An ultrahigh-resolution Orbitrap mass spectrometer coupled by a chemical ionization interface (CI-Orbitrap) has emerged as a novel tool, which combines advantages of ultra-high mass resolving power ($m/\Delta m$ ≈140 000) and minimal fragmentation from soft atmospheric pressure ionization.[36,37] The experiment setup was shown in Figure S3, where NaI-containing droplets were produced by a commercial atomizer or our home-made mist chamber and then removed by a hydrophobic PTFE membrane filter to allow a particle-free measurement of the remaining gas phase. Since CH_2Br_2 was used to produce reagent ions, $I_{2(g)}$ was detected as bromide-adduct such as $^{79}Br(I_2)^-$ and $^{81}Br(I_2)^-$, with their ratio consistent with the theoretical isotope prediction (Figure S4). We also semi-calibrated the instrument by introducing a known quantity of I_2 vapor into the CI-Orbitrap. The instrument showed good linear response for $I_{2(g)}$ at the ppt level (Text S3 and Figure S5). The data were processed using the Xcalibur 2.2 software (Thermo Scientific), and the selected ions (i.e., m/z = 332.7278 for $^{79}Br(I_2)^-$, m/z = 334.7258 for $^{81}Br(I_2)^-$) were exported with a mass tolerance of 10 ppm. For consistency, all $I_{2(g)}$ intensity reported in this study was shown as $^{79}Br(I_2)^-$ and detected at m/z = 332.7278. More detailed information about the CI-Orbitrap can be found elsewhere.[36,37]

Results and Discussion

Spontaneous I_3^- production from I^--containing droplets

We carried out experiments in microdroplets (1−10 μm); a few experiments investigated iodide oxidation at macroscopic aqueous interfaces as well. The microdroplet experiments used two droplet sources. In the first one, a home-made mist chamber, NaI-containing microdroplets were produced by spraying a 100 mM NaI bulk solution using various bath gases. The mist chamber was operated in a recirculation mode (Figure S2A), where the microdroplets continuously impacted on a membrane filter and dropped back into the bulk solution before being resprayed. Under such recycling conditions, any possible reaction products in the reservoir bulk water of the mist chamber accumulate over time. The reservoir bulk solution was analyzed for the appearance of I_3^- by UV-Vis spectroscopy, typically every hour. Figure 1A displays the absorption spectrum of I_3^- and its precursors; Figure 1B clearly indicates an increase of absorbance of I_3^- at ~352 nm after spraying a 100 mM NaI solution for 7 h using synthetic air (20% O_2 + 80% N_2) as the bath gas.

Interestingly, when such experiments are performed under nitrogen instead of synthetic air, Figure 1B shows that the increase of absorbance at ~352 nm is reduced, highlighting a possible role of oxygen in the observed chemistry. Normally, iodide is not oxidized by molecular oxygen in solution or gas phase. To test whether our observation relates to electron capture by oxygen at the air-water interface, 2-chloroethanol (C_2H_4ClOH) - a strong electron scavenger - was added to the pure nitrogen gas flow and gave rise to a notable increase of the I_3^- production, as illustrated in Figure 1B.

In order to test whether the observed iodide activation is dependent on the spraying procedure, we employed a commercial atomizer (TSI 3076), rather than the mist chamber, to nebulize the same NaI solution into microdroplets, which were subsequently trapped in two tandem glass bottles for UV-Vis measurement. Figure S2B illustrates the experimental arrangement used for these experiments. As shown in Figure 1C, we also observed the peak at ~352 nm in this case, indicating formation of I_3^- in the microdroplets collected using four different spraying gases. Again, adding oxygen or 2-chloroethanol to the nitrogen gas yielded much greater amounts of I_3^- product than using pure nitrogen. Compared with the first vessel, the microdroplets trapped in the second vessel generally showed a higher absorbance at ~352 nm due to a longer residence time.

Finally, we demonstrated that iodide anions are oxidized even on flat macroscopic surfaces in the dark. For this purpose, one glass bottle (30 mL size) was filled with 3 mL volume of NaI-

containing solution with a macroscopic air-water interface (surface area of ca. 8.3 cm^2), and another identical glass bottle was fully filled with the same solution with no head-space (i.e., with no air-water interface) (Figure S6). Under such conditions, I_3^- production was observed after several days from the solution that had a macroscopic air-water interface, while no I_3^- formation was observed in the solution with no interface, even days after preparing the stock solution (Figure S6). These experiments confirm that iodide oxidation does not occur in bulk solution, but requires an interface, and that it is not driven by impurities present in our water supply or in the chemicals used.

The enhanced iodide activation due to the addition of electron scavengers suggests the involvement of free electrons in the mechanism. This in turn implies that I^- may be oxidized to produce a free electron according to (E1), in a manner similar to that previously suggested for the dissociation of hydroxide anions (OH^-) into OH radicals and electrons under the naturally formed electric field (~10^9 V m^{-1}) at the air-water interface of microdroplets.[6,9,13–15,38]

$$I^- \overset{\text{electric field}}{\rightleftharpoons} I\cdot + e^- \qquad \text{(E1)}$$

Similar to OH^- as initially proposed by Kloss,[13] the forward step in E1 is suggested to be a charge separation process induced by an interfacial electric field, and hence it should not be regarded as an oxidation process that costly in energy. For instance, iodide is serving a typical example for investigating charge-transfer-to-solvent (CTTS) transitions and the corresponding solvation transitions have been investigated.[39] However, the transition is typically triggered by appropriate UV light, in contrast to what is suggested here. The electron affinity of the iodine atom is determined as 3.059 eV.[40] It is known that solvation shells do differ between the bulk and the interfacial region, and that this may facilitate or promote some redox reactions.[41–43] Here specifically, modified solvation processes at the interface will affect the equilibrium E1. If the electron is scavenged, the equilibrium in (E1) will be shifted to the right and enhance iodide activation. Once produced, the atomic iodine may react through a sequence of different reactions (E2-E5) producing I_2, I_2^- and finally I_3^-, of which many I_2^- may decay back to I^- (E6),[44] according to:

$$I\cdot + I\cdot \rightleftharpoons I_{2(aq)} \qquad \text{(E2)}$$

$$I\cdot + I^- \rightleftharpoons I_2^- \qquad \text{(E3)}$$

$$I_2^- + I^- \rightleftharpoons I_3^- \qquad \text{(E4)}$$

$$I_{2(aq)} + I^- \rightleftharpoons I_3^- \qquad \text{(E5)}$$

$$I_2^- + I_2^- \rightleftharpoons I_3^- + I^- \quad \text{(E6)}$$

Under pure nitrogen, the solvated electron generated in E1 can recombine on an approximately hundred picosecond timescale with the nearby I radical due to a solvent cage effect,[45] resulting in a null cycle. By contrast, enhanced I_3^- formation was observed when an electron scavenger such as $C_2H_4ClOH_{(g)}$, $O_{2(g)}$ or $N_2O_{(g)}$ was added to the pure N_2 gas spraying flow,[46,47] either in the mist chamber (Figure 1B and Figure S7A) or using a commercial atomizer (Figure 1C and Figure S8). Note that $C_2H_4ClOH_{(g)}$ has high solubility in water, which can lower the solution pH by forming HCl through hydrolysis of the dissolved $C_2H_4ClOH_{(g)}$, as illustrated in Figure S7D-E. The lowered pH may also affect the electron lifetime in solution. In addition, by dissolving over time in the aqueous solution, C_2H_4ClOH may also change the physical characteristics of the nebulized aerosol droplets due to changes in colligative properties and specific molecular interactions. However, our observation of enhanced I_3^- production in the presence of $O_{2(g)}$ and $N_2O_{(g)}$, neither of which is strongly soluble, gives strong support to electron capture at the air-aqueous interface as being a key driver of I_3^- production (see Text S4 and Figure S8).

The presence of an electron scavenger will shift the equilibrium in E1, allowing I atoms to live sufficiently long to produce I_2, I_2^- as well as I_3^-, via E2–E6 above. This reaction scheme gives a plausible explanation for the observation of I_3^- formation. As many of such intermediates decay back to iodide, our observations represent only a lower limit to the actual activation of the iodide anion. It is worth mentioning that a recent work by Xing et al.[28] also reported similar I_3^- formation from spraying NaI bulk solution into microdroplets, and they proposed that the oxidation of iodide was explained by spontaneous production of OH radicals at the interface and subsequent OH-oxidation chemistry. Given the ubiquitous interfacial production of OH radicals,[9] this pathway is certainly taking place as well under our conditions, as the experimental approach is overall similar. However, we do suggest that this OH-initiated iodide oxidation should be regarded as minor. In fact, the addition of an organic compound, in large excess and acting as an OH radical scavenger, should prevent the formation of I_2 or I_3^-. By contrast, the addition of 2-chloroethanol did not prevent the formation of these products but rather enhanced their appearance, showing indeed that the key element in this chemistry is the electron trapping process that displaces equilibrium E1 to the right. Additionally, our observation of gas phase I_2 formation and Langmuir–Hinshelwood behaviour (vide infra) suggest that spontaneous iodide activation is more likely driven by a surface-mediated process involving the loss of free electrons (E1).

I_3^- production rates (in nmol h^{-1}; see Text S5) measured under different spraying gases were summarized in Figure 2A. The clear evidence for activation of iodide seen in the droplets was not observed in bulk solution, and was enhanced in the presence of gas phase electron scavengers. These observations are consistent with a surface-mediated mechanism taking place at the air-water interface. This conjecture is supported by the dependence of I_3^- production on the bulk iodide concentration. Figure 2B shows that the I_3^- production rate does not depend linearly on bulk iodide concentration (as expected for a first order bulk process), but exhibits limiting behavior, with a linear dependence at lower I^- concentrations (0.1−20 mM), and reaching a plateau at higher I^- concentrations (20−100 mM). The detailed results for each individual mist chamber experiment are summarized in Figure S9 and Table S1. Such a relationship between the I_3^- production rate and the NaI bulk concentration is well represented by a Langmuir–Hinshelwood model, which is specific for surface driven processes.[48–51] This idea is explored further below. Altogether, these indications are strongly supportive of an interfacial oxidation of iodide anion giving rise to I_3^- production.

Release of interfacial I_2 into the gas phase

Molecular iodine is only moderately soluble in water, with a Henry's law constant of ca. 2.8 M atm^{-1} at room temperature.[52] As a consequence, if I_2 production occurs at the air-water interface, one would expect a significant fraction of that compound to desorb into the gas phase. To test whether gaseous iodine is produced at the droplet surface, we performed direct measurement of $I_{2(g)}$ using an online chemical ionization orbitrap (CI-Orbitrap) instrument, with bromide as reagent ion.

As shown in Figure 3A, we observed clear steady-state $I_{2(g)}$ signal (detected as bromide-adduct such as $^{79}Br(I_2)^-$) when atomizing a 100 mM NaI solution under N_2 or pure air, while a 100 mM $(NH_4)_2SO_4$ solution nebulized by the same procedure led to signal at the level of instrumental background. Compared with the results using N_2 as carrier gas, enhanced $I_{2(g)}$ signal was observed using pure air (Figure 3A−B and Figure S10A−B), consistent with the observations of enhanced I_3^- production in the presence of $O_{2(g)}$ discussed above. This comparison reinforces the fact that electron scavengers such as oxygen can play an important promotion role for the interfacial iodide activation. Figure 3C and Figure S10C show the $I_{2(g)}$ signal as a function of pH of a 10 mM NaI bulk solution. The production of I_2 seems to be more efficient under acidic conditions, again similar to what we see for I_3^- production in Figure S7C. Such pH dependence agrees with previous findings that abundant protons (H^+) at lower pH could enhance the production of $I^-_{3(aq)}$ and $I_{2(g)}$.[33,53] As shown in Figure 3D, the $I_{2(g)}$ signal also shows a non-linear dependence on the bulk NaI concentration, similar to what is shown above in Figure 2B for I_3^- production. This is compelling evidence to support the proposal that both spontaneous $I_{2(g)}$ production and I_3^- production via iodide activation take place

as an interfacial process. Such Langmuir–Hinshelwood behaviour also rules out the potential iodide activation route from interfacial production of H_2O_2. For instance, if I_2 would arise from the titration of iodide by H_2O_2, then the amount of I_2 produced should not depend on the I^- concentration due to the great excess of I^- to H_2O_2, which does not agree with the above observation in this study.

The CI-Orbitrap instrument demonstrated a linear response to different $I_{2(g)}$ concentrations, and here was only calibrated for semi-quantitative purposes (see Figure S5 and Text S3 for details). The corresponding semi-quantitative $I_{2(g)}$ concentrations for all experimental conditions tested here are summarized in Table S3. Total surface area concentrations could be calculated based on the droplet size distribution measured at the output of the atomizer or mist chamber (Figure S2C−E), respectively. As shown in Table S4, the surface area normalized $I_{2(g)}$ concentrations were calculated to be in the range of $2-8\times10^{15}$ molec m^{-2} for droplets produced from atomizer and mist chamber respectively, which agrees in between within a factor of 4.

Langmuir-Hinshelwood behaviour

The dependence of product formation on bulk iodide concentration is consistent between both aqueous phase I_3^- production (Figure 2B) and gas phase $I_{2(g)}$ production (Figure 3D). This implies that the production of both species has the same dependence on the presence of iodide anions at the air-water interface. In order to describe this process by a Langmuir–Hinshelwood kinetic model, we normalize all the production rates to their maxima, and plot these as a function of bulk NaI concentration in Figure 4, fitting the data to a Langmuir–Hinshelwood equation (1):

$$\text{normalized } I_3^- \text{ and } I_{2(g)} \text{ production} = \frac{A[I^-_{aq}]}{B+[I^-_{aq}]} = \frac{A[I^-_{aq}]}{1/K_{ads}+[I^-_{aq}]} \quad (1)$$

In this equation, $[I^-_{aq}]$ is the bulk concentration of iodide; parameter A represents the maximum observed rate; parameter B represents the ratio of the desorption to adsorption rate constants for I^- adsorption from the bulk solution to the interface, which is equivalent to the inverse of equilibrium constant of I^-_{aq} for surface adsorption (K_{ads}).[49,50]

By applying a Langmuir–Hinshelwood fit to the combined data in Figure 4, we obtain an adsorption constant K_{ads} of 295±100 M^{-1} for I^- partitioning from bulk to the interface. Note that this does not represent a true thermodynamic equilibrium constant, as we have ignored activity coefficient and the surface standard state is not defined. However, comparing this value to other similar analyses shows reasonable agreement within a factor of 4−13, with the reported K_{ads} values (i.e., 23±3 M^{-1} and 70±16 M^{-1}), from analysis of the heterogeneous reaction between $O_{3(g)}$ and NaI solution.[50,51]

Atmospheric implications

It is worth mentioning that some previous studies also reported $I_{3(aq)}^-$ and $I_{2(g)}$ production as a result of the addition of an external trigger i.e., ozone, irradiation, catalyst, etc.[33,34,53,54] We observed spontaneous I_3^- and $I_{2(g)}$ production from NaI droplets through an iodide activation process that does not require catalysts, external voltages, oxidants or irradiation. This represents a previously unknown source of reactive iodine species. Our results suggest that such spontaneous dark production of I_3^- and $I_{2(g)}$ is an interfacial process, which can be well described using a Langmuir–Hinshelwood formalism. The production of I_3^- and $I_{2(g)}$ is strongly affected by the presence of electron scavengers such as N_2O, O_2 or C_2H_4ClOH, consistent with oxidation of iodide at the interface.

We propose that this spontaneous iodide activation could be induced by the strong electric field ($\sim 10^9$ V m^{-1}) which is thought to be formed naturally at the air-water interface of microdroplets.[14,15] However, molecular dynamics simulations show large fluctuations across the interface due to partial solvation effect and the associated variation of the solvent electrostatic potential, which suggests the incomplete and large uncertainty in the current understanding of interfacial electric field.[55,56] Similar to the recent observation of spontaneous H_2O_2 and OH radical production at the interface of microdroplets,[9,38] we hypothesize that such a high electric field can dissociate iodide anions into iodine atoms and electrons (e^-) (E1), following by the formation of reactive iodine species (I and I_2), which can further accommodate into the aqueous phase or be released into the gas phase and then potentially trigger more iodine-related reactions with other compounds. For instance, the aqueous iodine species may react with dissolved organic matter in the sea-surface microlayer to produce organo-iodine species,[21,23] while the interfacial released $I_{2(g)}$ could deplete tropospheric O_3, initiate new particle formation and oxidize hydrocarbons.[17,57,58] The Supporting Information (Text S6 and Figures S11−S12) gives details of some preliminary experiments that show new particle formation by reaction of the I_2 released from droplet surfaces with ozone under visible irradiation.

Supporting Information

The Supporting Information includes additional experimental details, materials and methods, and further results from mist chamber and atomizer experiments, $I_{2(g)}$ calibration with CI-Orbitrap and aerosol flow tube (AFT) experiments.

Acknowledgment

This study was supported by the European Research Council under the Horizon 2020 research and innovation programme / ERC Grant Agreement 101052601 — SOFA. TA and YG acknowledge the financial support from the National Natural Science Foundation of China (42020104001 and 42377221).

Author Information

Yunlong Guo and Kangwei Li contributed equally to this work.

References

(1) George, C.; Ammann, M.; D'Anna, B.; Donaldson, D. J.; Nizkorodov, S. A. Heterogeneous photochemistry in the atmosphere. *Chem. Rev.* **2015,** *115*, 4218-4258.

(2) Pillar-Little, E.; Guzman, M. An overview of dynamic heterogeneous oxidations in the troposphere. *Environments* **2018,** *5*, 104.

(3) Ruiz-Lopez, M. F.; Francisco, J. S.; Martins-Costa, M. T. C.; Anglada, J. M. Molecular reactions at aqueous interfaces. *Nat. Rev. Chem.* **2020,** *4,* 459-475.

(4) Rossignol, S.; Tinel, L.; Bianco, A.; Passananti, M.; Brigante, M.; Donaldson, D. J.; George, C. Atmospheric photochemistry at a fatty acid-coated air-water interface. *Science* **2016,** *353*, 699-702.

(5) Lee, J. K.; Samanta, D.; Nam, H. G.; Zare, R. N. Micrometer-sized water droplets induce spontaneous reduction. *J. Am. Chem. Soc.* **2019,** *141*, 10585-10589.

(6) Lee, J. K.; Walker, K. L.; Han, H. S.; Kang, J.; Prinz, F. B.; Waymouth, R. M.; Nam, H. G.; Zare, R. N. Spontaneous generation of hydrogen peroxide from aqueous microdroplets. *P. Natl. Acad. Sci. USA* **2019,** *116,* 19294-19298.

(7) Lee, J. K.; Han, H. S.; Chaikasetsin, S.; Marron, D. P.; Waymouth, R. M.; Prinz, F. B.; Zare, R. N. Condensing water vapor to droplets generates hydrogen peroxide. *P. Natl. Acad. Sci. USA* **2020,** *117*, 30934-30941.

(8) Gong, C.; Li, D.; Li, X.; Zhang, D.; Xing, D.; Zhao, L.; Yuan, X.; Zhang, X. Spontaneous reduction-induced degradation of viologen compounds in water microdroplets and its inhibition by host-guest complexation. *J. Am. Chem. Soc.* **2022,** *144*, 3510-3516.

(9) Li, K.; Guo, Y.; Nizkorodov, S. A.; Rudich, Y.; Angelaki, M.; Wang, X.; An, T.; Perrier, S.; George, C. Spontaneous dark formation of OH radicals at the interface of aqueous atmospheric droplets. *P. Natl. Acad. Sci. USA* **2023,** *120*, e2220228120.

(10) Musskopf, N. H.; Gallo Jr, A.; Zhang, P.; Petry, J.; Mishra, H. The air–water interface of water microdroplets formed by ultrasonication or condensation does not produce H_2O_2. *J. Phys. Chem. Lett.* **2021,** *12*, 11422-11429.

(11) Nguyen, D.; Nguyen, S. C. Revisiting the effect of the air–water interface of ultrasonically atomized water microdroplets on H_2O_2 formation. *J. Phys. Chem. B* **2022,** *126*, 3180-3185.

(12) Nguyen, D.; Lyu, P.; Nguyen, S. C. Experimental and thermodynamic viewpoints on claims of a spontaneous H_2O_2 formation at the air–water interface. *J. Phys. Chem. B* **2023,** *127*, 2323-2330.

(13) Kloss, A. I. Electron-radical dissociation and the water activation mechanism. *Doklady Akademii Nauk Sssr* **1988,** *303*, 1403-1407.

(14) Xiong, H.; Lee, J. K.; Zare, R. N.; Min, W. Strong electric field observed at the interface of aqueous microdroplets. *J. Phys. Chem. Lett.* **2020,** *11*, 7423-7428.

(15) Hao, H.; Leven, I.; Head-Gordon, T. Can electric fields drive chemistry for an aqueous microdroplet? *Nat. Commun.* **2022,** *13*, 280.

(16) Heindel, J. P.; Hao, H.; LaCour, R. A.; Head-Gordon, T. Spontaneous formation of hydrogen peroxide in water microdroplets. *J. Phys. Chem. Lett.* **2022,** *13*, 10035-10041.

(17) Carpenter, L. J. Iodine in the marine boundary layer. *Chem. Rev.* **2003,** *103*, 4953-4962.

(18) Carpenter, L. J.; MacDonald, S. M.; Shaw, M. D.; Kumar, R.; Saunders, R. W.; Parthipan, R.; Wilson, J.; Plane, J. M. C. Atmospheric iodine levels influenced by sea surface emissions of inorganic iodine. *Nat. Geo.* **2013,** *6*, 108-111.
(19) O'Dowd, C. D.; Hoffmann, T. Coastal new particle formation: A review of the current state-of-the-art. *Environ. Chem.* **2005,** *2*, 245-255.
(20) Huang, R.-J.; Hoffmann, T.; Ovadnevaite, J.; Laaksonen, A.; Kokkola, H.; Xu, W.; Xu, W.; Ceburnis, D.; Zhang, R.; Seinfeld, J. H.; O'Dowd, C. Heterogeneous iodine-organic chemistry fast-tracks marine new particle formation. *P. Natl. Acad. Sci. USA* **2022,** *119*, e2201729119.
(21) Carpenter, L. J.; Chance, R. J.; Sherwen, T.; Adams, T. J.; Ball, S. M.; Evans, M. J.; Hepach, H.; Hollis, L. D. J.; Hughes, C.; Jickells, T. D.; Mahajan, A.; Stevens, D. P.; Tinel, L.; Wadley, M. R. Marine iodine emissions in a changing world. *Proc. R. Soc. A* **2021,** *477*, 20200824.
(22) Koenig, T. K.; Baidar, S.; Campuzano-Jost, P.; Cuevas, C. A.; Dix, B.; Fernandez, R. P.; Guo, H.; Hall, S. R.; Kinnison, D.; Nault, B. A.; Ullmann, K.; Jimenez, J. L.; Saiz-Lopez, A.; Volkamer, R. Quantitative detection of iodine in the stratosphere. *P. Natl. Acad. Sci. USA* **2020,** *117*, 1860-1866.
(23) Simpson, W. R.; Brown, S. S.; Saiz-Lopez, A.; Thornton, J. A.; Glasow, R. Tropospheric halogen chemistry: Sources, cycling, and impacts. *Chem. Rev.* **2015,** *115*, 4035-4062.
(24) Carpenter, L. J.; Nightingale, P. D. Chemistry and release of gases from the surface ocean. *Chem. Rev.* **2015,** *115*, 4015-4034.
(25) Tham, Y. J.; He, X.-C.; Li, Q.; Cuevas, C. A.; Shen, J.; Kalliokoski, J.; Yan, C.; Iyer, S.; Lehmusjarvi, T.; Jang, S.; Thakur, R. C.; Beck, L.; Kemppainen, D.; Olin, M.; Sarnela, N.; Mikkila, J.; Hakala, J.; Marbouti, M.; Yao, L.; Li, H.; Huang, W.; Wang, Y.; Wimmer, D.; Zha, Q.; Virkanen, J.; Spain, T. G.; O'Doherty, S.; Jokinen, T.; Bianchi, F.; Petaja, T.; Worsnop, D. R.; Mauldin III, R. L.; Ovadnevaite, J.; Ceburnis, D.; Maier, N. M.; Kulmala, M.; O'Dowd, C.; Maso, M. D.; Saiz-Lopez, A.; Sipila, M. Direct field evidence of autocatalytic iodine release from atmospheric aerosol. *P. Natl. Acad. Sci. USA* **2021,** *118*, e2009951118.
(26) Vogt, R.; Sander, R.; von Glasow, R.; Crutzen, P. J. Iodine chemistry and its role in halogen activation and ozone loss in the marine boundary layer: A model study. *J. Atmos. Chem.* **1999,** *32*, 375-395.
(27) Pillar-Little, E. A.; Guzman, M. I.; Rodriguez, J. M. Conversion of iodide to hypoiodous acid and iodine in aqueous microdroplets exposed to ozone. *Environ. Sci. Technol.* **2013,** *47*, 10971-10979.
(28) Xing, D.; Yuan, X.; Liang, C.; Jin, T.; Zhang, S.; Zhang, X. Spontaneous oxidation of I^- in water microdroplets and its atmospheric implications. *Chem. Commun.* **2022,** *58*, 12447-12450.
(29) Saiz-Lopez, A.; Plane, J. M. C.; Baker, A. R.; Carpenter, L. J.; Glasow, R. V.; Martín, J. C. C.; McFiggans, G.; Saunders, R. W. Atmospheric chemistry of iodine. *Chem. Rev.* **2011,** *112*, 1773-1804.
(30) Fournier, M. C.; Falk, L.; Villermaux, J. A new parallel competing reaction system for assessing micromixing efficiency-Experimental approach. *Chem. Eng. Sci.* **1996,** *51*, 5053-5064.
(31) Kireev, S. V.; Shnyrev, S. L. Study of molecular iodine, iodate ions, iodide ions, and triiodide ions solutions absorption in the UV and visible light spectral bands. *Laser Phys.* **2015,** *25*, 075602.
(32) Dixon, S. L.; Jurs, P. C. Estimation of pKa for organic oxyacids using calculated atomic charges. *J. Comput. Chem.* **1993,** *14*, 1460-1467.

(33) Kim, K.; Yabushita, A.; Okumura, M.; Saiz-Lopez, A.; Cuevas, C. A.; Blaszczak-Boxe, C. S.; Min, D. W.; Yoon, H.-I.; Choi, W. Production of molecular iodine and tri-iodide in the frozen solution of iodide: Implication for polar atmosphere. *Environ. Sci. Technol.* **2016,** *50*, 1280-1287.

(34) Halfacre, J. W.; Shepson, P. B.; Pratt, K. A., pH-dependent production of molecular chlorine, bromine, and iodine from frozen saline surfaces. *Atmos. Chem. Phys.* **2019,** *19*, 4917-4931.

(35) Wang, M.; He, X.-C.; Finkenzeller, H.; Iyer, S.; Chen, D.; Shen, J.; Simon, M.; Hofbauer, V.; Kirkby, J.; Curtius, J.; Maier, N.; Kurtén, T.; Worsnop, D. R.; Kulmala, M.; Rissanen, M.; Volkamer, R.; Tham, Y. J.; Donahue, N. M.; Sipilä, M. Measurement of iodine species and sulfuric acid using bromide chemical ionization mass spectrometers. *Atmos. Meas. Tech.* **2021,** *14*, 4187-4202.

(36) Riva, M.; Ehn, M.; Li, D.; Tomaz, S.; Bourgain, F.; Perrier, S.; George, C. CI-Orbitrap: An analytical instrument to study atmospheric reactive organic species. *Anal. Chem.* **2019,** *91*, 9419-9423.

(37) Riva, M.; Brüggemann, M.; Li, D.; Perrier, S.; George, C.; Herrmann, H.; Berndt, T. Capability of CI-Orbitrap for gas-phase analysis in atmospheric chemistry: A comparison with the CI-APi-TOF technique. *Anal. Chem.* **2020,** *92*, 8142-8150.

(38) Zhao, L.; Song, X.; Gong, C.; Zhang, D.; Wang, R.; Zare, R. N.; Zhang, X. Sprayed water microdroplets containing dissolved pyridine spontaneously generate pyridyl anions. *P. Natl. Acad. Sci. USA* **2022,** *119*, e2200991119.

(39) Bhattacharyya, D.; Mizuno, H.; Rizzuto, A. M.; Zhang, Y.; Saykally, R. J.; Bradforth, S. E. New insights into the charge-transfer-to-solvent spectrum of aqueous iodide: Surface versus bulk. *J. Phys. Chem. Lett.* **2020,** *11,* 1656-1661.

(40) Peláez, R. J.; Blondel, C.; Delsart, C.; Drag, C. Pulsed photodetachment microscopy and the electron affinity of iodine. *J. Phys B: At. Mol. Opt.* **2009,** *42*, 125001.

(41) Kong, X.; Castarede, D.; Thomson, E. S.; Boucly, A.; Artiglia, L.; Ammann, M.; Gladich, I.; Pettersson, J. B. C. A surface-promoted redox reaction occurs spontaneously on solvating inorganic aerosol surfaces. *Science* **2021,** *374*, 747-752.

(42) Ammann, M.; Artiglia, L. Solvation, surface propensity, and chemical reactions of solutes at atmospheric liquid-vapor interfaces. *Acc. Chem. Res.* **2022,** *55*, 3641-3651.

(43) Fauré, N.; Chen, J.; Artiglia, L.; Ammann, M.; Bartels-Rausch, T.; Li, J.; Liu, W.; Wang, S.; Kanji, Z. A.; Pettersson, J. B. C.; Thomson, E. S.; Kong, X. Unexpected behavior of chloride and sulfate ions upon surface solvation of martian salt analogue. *ACS Earth Space Chem.* **2023,** *7*, 350-359.

(44) Nishiyama, Y.; Terazima, M.; Kimura, Y. Ultrafast relaxation and reaction of diiodide anion after photodissociation of triiodide in room-temperature ionic liquids. *J. Phys. Chem. B* **2012,** *116*, 9023-9032.

(45) Sagar, D. M.; Bain, C. D.; Verlet, J. R. R. Hydrated electrons at the water/air interface. *J. Am. Chem. Soc.* **2010,** *132*, 6917-6919.

(46) Zechner, J.; Köhler, G.; Getoff, N.; Tatischeff, I.; Klein, R. Wavelength effects on the photoprocesses of indole and derivatives in solution. *Photochem. Photobiol.* **1981,** *34*, 163-168.

(47) Zepp, R. G.; Braun, A. M.; Hoigne, J.; Leenheer, J. A. Photoproduction of hydrated electrons from natural organic solutes in aquatic environments. *Environ. Sci. Technol.* **1987,** *21*, 485-490.

(48) Pöschl, U.; Letzel, T.; Schauer, C.; Niessner, R. Interaction of ozone and water vapor with spark discharge soot aerosol particles coated with benzo[*a*]pyrene: O_3 and H_2O adsorption,

benzo[*a*]pyrene degradation, and atmospheric implications. *J. Phys. Chem. A* **2001,** *105*, 4029-4041.

(49) Mmereki, B. T.; Donaldson, D. J. Direct observation of the kinetics of an atmospherically important reaction at the air-aqueous interface. *J. Phys. Chem. A* **2003,** *107*, 11038-11042.

(50) Reeser, D. I.; Donaldson, D. J. Influence of water surface properties on the heterogeneous reaction between $O_{3(g)}$ and $I^-_{(aq)}$. *Atmos. Environ.* **2011,** *45*, 6116-6120.

(51) Wren, S. N.; Donaldson, D. J. Glancing-angle Raman spectroscopic probe for reaction kinetics at water surfaces. *Phys. Chem. Chem. Phys.* **2010,** *12*, 2648-2654.

(52) Sander, R. Compilation of Henry's law constants (version 4.0) for water as solvent. *Atmos. Chem. Phys.* **2015,** *15*, 4399-4981.

(53) Hayase, S.; Yabushita, A.; Kawasaki, M.; Enami, S.; Hoffmann, M. R.; Colussi, A. J. Weak acids enhance halogen activation on atmospheric water's surfaces. *J. Phys. Chem. A* **2011,** *115*, 4935-4940.

(54) Watanabe, K.; Matsuda, S.; Cuevas, C. A.; Saiz-Lopez, A.; Yabushita, A.; Nakano, Y. Experimental determination of the photooxidation of aqueous I^- as a source of atmospheric I_2. *ACS Earth Space Chem.* **2019,** *3*, 669-679.

(55) Martins-Costa, M. T. C.; Anglada, J. M.; Francisco, J. S.; Ruiz-Lopez, M. F. Reactivity of atmospherically relevant small radicals at the air–water interface. *Angew. Chem. Int. Ed.* **2012,** *51,* 5413–5417.

(56) Martins-Costa, M. T. C.; Ruiz-López, M. F. Electrostatics and chemical reactivity at the air–water interface. *J. Am. Chem. Soc.* **2023,** *145*, 1400-1406.

(57) Sherwen, T.; Schmidt, J. A.; Evans, M. J.; Carpenter, L. J.; Großmann, K.; Eastham, S. D.; Jacob, D. J.; Dix, B.; Koenig, T. K.; Sinreich, R.; Ortega, I.; Volkamer, R.; Saiz-Lopez, A.; Prados-Roman, C.; Mahajan, A. S.; Ordóñez, C. Global impacts of tropospheric halogens (Cl, Br, I) on oxidants and composition in GEOS-Chem. *Atmos. Chem. Phys.* **2016,** *16*, 12239-12271.

(58) McFiggans, G.; Bale, C. S. E.; Ball, S. M.; Beames, J. M.; Bloss, W. J.; Carpenter, L. J.; Dorsey, J.; Dunk, R.; Flynn, M. J.; Furneaux, K. L.; Gallagher, M. W.; Heard, D. E.; Hollingsworth, A. M.; Hornsby, K.; Ingham, T.; Jones, C. E.; Jones, R. L.; Kramer, L. J.; Langridge, J. M.; Leblanc, C.; LeCrane, J. P.; Lee, J. D.; Leigh, R. J.; Longley, I.; Mahajan, A. S.; Monks, P. S.; Oetjen, H.; Orr-Ewing, A. J.; Plane, J. M. C.; Potin, P.; Shillings, A. J. L.; Thomas, F.; von Glasow, R.; Wada, R.; Whalley, L. K.; Whitehead, J. D. Iodine-mediated coastal particle formation: An overview of the Reactive Halogens in the Marine Boundary Layer (RHaMBLe) Roscoff coastal study. *Atmos. Chem. Phys.* **2010,** *10*, 2975-2999.

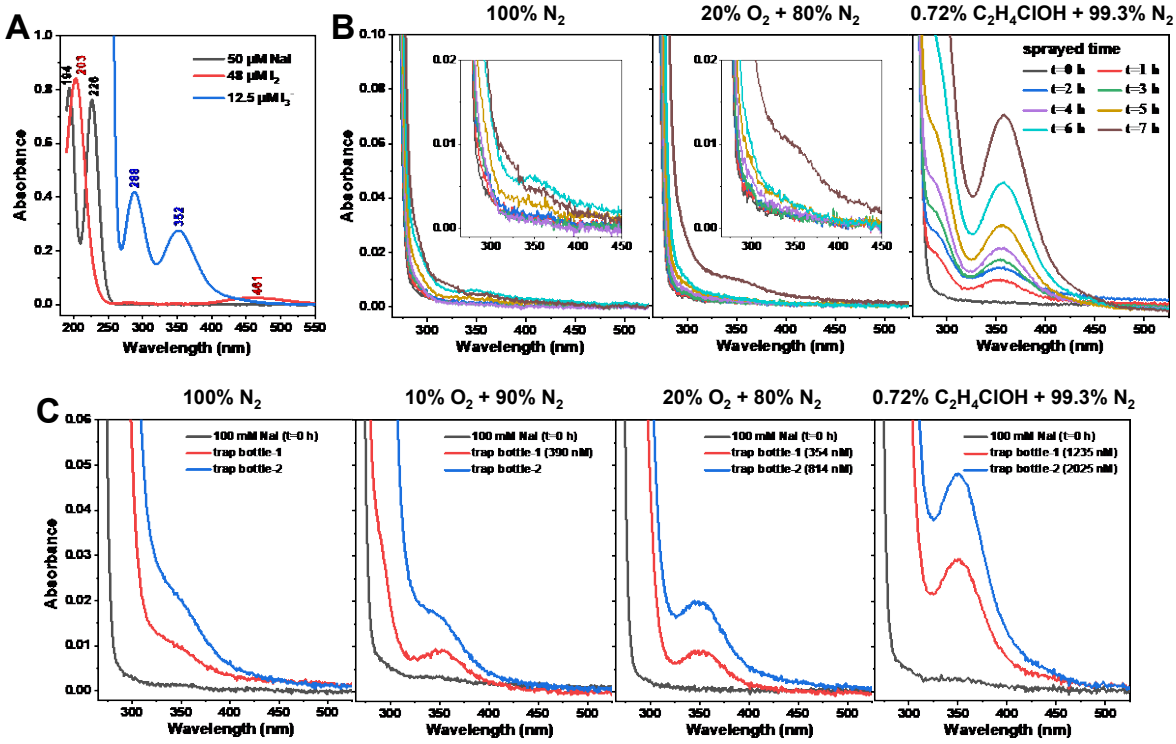

Figure 1. Spontaneous I_3^- production from NaI droplets based on UV-Vis measurement. (A) The absorption spectra of NaI, $I_{2(aq)}$ and I_3^- standard solutions at selected concentrations. (B) Time-dependent absorption spectra for bulk solution (100 mM NaI, pH=6.2) in mist chamber experiment under different spray gases (see inset for enlarged spectra), including pure N_2, 20% O_2 + 80% N_2, and 0.72% $C_2H_4ClOH_{(g)}$ in N_2. (C) The absorption spectra for droplets produced by atomizing the same 100 mM NaI bulk solution under different carrier gases, which were collected as condensing liquid in two tandem bottles as shown in Figure S2B.

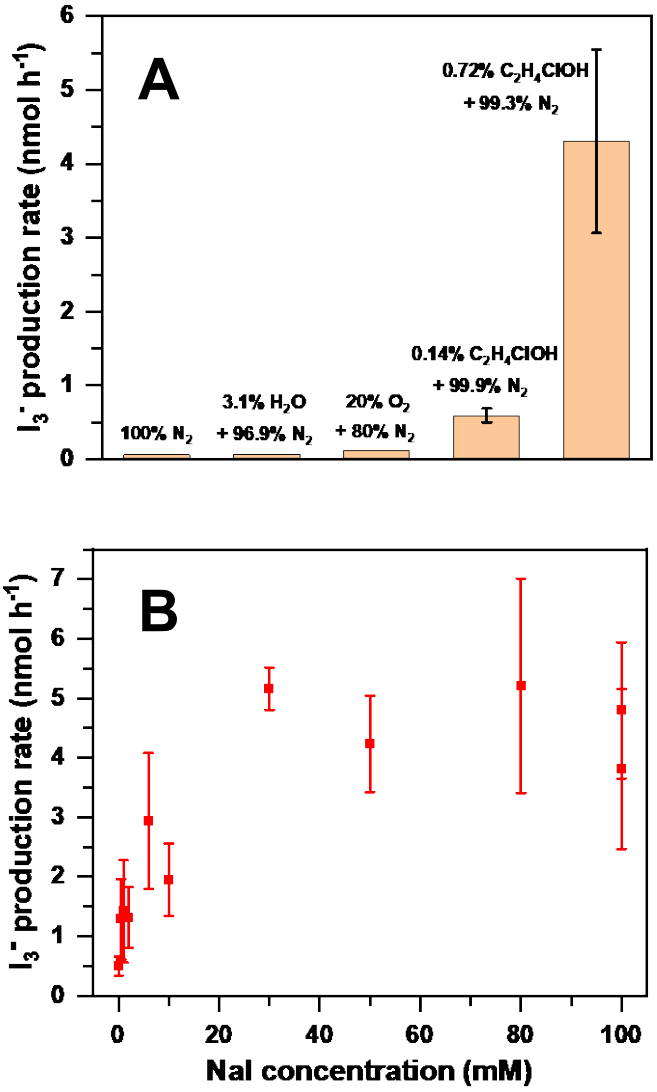

513

514 **Figure 2.** I_3^- production rate from mist chamber experiments under different conditions. (A) Fixed
515 NaI bulk solution (100 mM) under different spraying gases. (B) Varied NaI bulk solution (0.1−100
516 mM) under the same spraying gas (0.72% $C_2H_4ClOH_{(g)}$ in N_2). Error bars represented standard
517 deviation (1σ) from 2–10 measurements from different spraying time (Tables S1−S2).

518

519

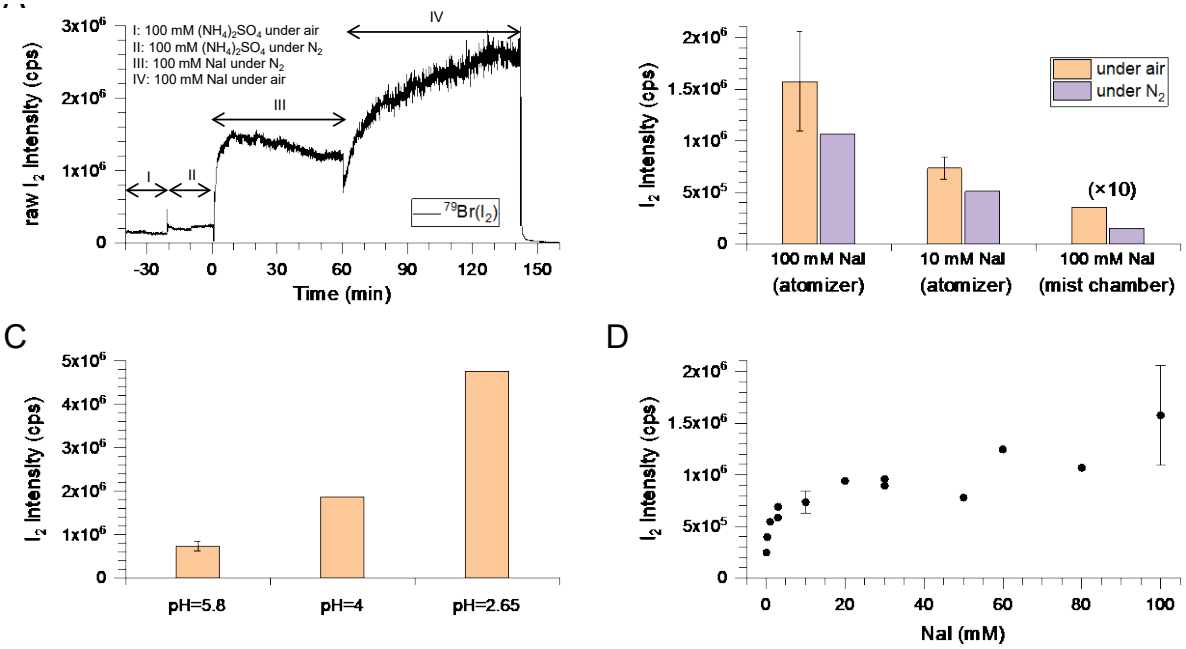

Figure 3. Direct $I_{2(g)}$ measurement from NaI-containing droplets under various experimental conditions. (A) Time-dependent raw $I_{2(g)}$ intensity measured at the output of atomizer by atomizing 100 mM NaI under N_2 and air, respectively. (B) $I_{2(g)}$ intensity measured at the output of atomizer or mist chamber with 100 mM or 10 mM NaI under air vs. N_2. (C) $I_{2(g)}$ intensity measured at the output of atomizer with 10 mM NaI under different solution pH. (D) $I_{2(g)}$ intensity measured at the output of atomizer as a function of bulk NaI concentration.

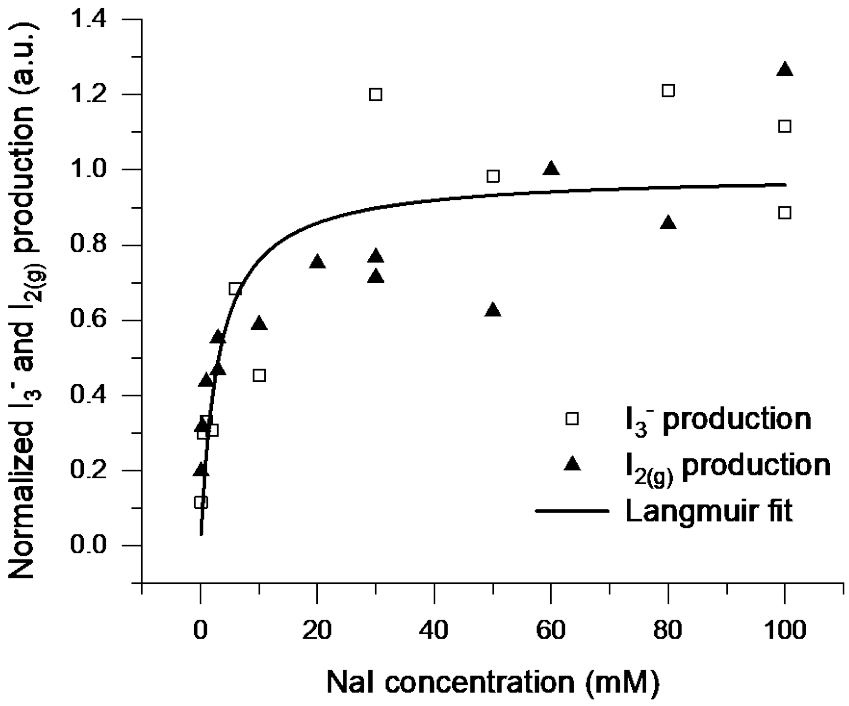

Figure 4. Observed I_3^- and $I_{2(g)}$ production from spontaneous iodide activation as a function of bulk NaI concentration. The data from Figure 2B and Figure 3D were normalized to their respective maxima and the combined data fit with a Langmuir–Hinshelwood model.